COBEM 2021 26th International Congress of Mechanical Engineering
November 22-26, 2021, Virtual Congress, Brazil

COB-2021-2154
COMPARATIVE STUDY OF BIOGENIC AND CHEMICAL SYNTHESIZED HYDROXYAPATITE FOR BIOMEDICAL APPLICATIONS

Marla Karolyne dos Santos Horta
Francisco José Moura
Pontifícia Universidade Católicado Rio de Janeiro, R. Marquês de São Vicente, 225 - Gávea, Rio de Janeiro - RJ, 22451-900
marla.horta@hotmail.com
moura@puc-rio.br

Marilza Sampaio Aguilar
Universidade Estácio de Sá, Rua Santanésia, 56 - Rio Comprido, Rio de Janeiro - RJ, 20261-180
aguilar.marilzas@gmail.com

José Brant de Campos
Universidade do Estado do Rio de Janeiro, Rua São Francisco Xavier, 524, 5° andar - Sala 5020 Bloco A, Maracanã, Rio de Janeiro
brant@uerj.br

Daniel Navarro da Rocha
R-crio Criogenia S.A., R. Cumarú, 204 - Alphaville Empresarial, Campinas - SP, 13098-324
dnr.navarro@gmail.com

Cecília Buzatto Westin
Universidade Estadual de Campinas, Av. Albert Einstein, 500 - Cidade Universitária, Campinas - SP, 13083-852
ceciliabwestin@gmail.com

Abstract. *The use of biogenic sources to obtain calcium phosphate compounds, mainly hydroxyapatite (HAp), is an excellent alternative to try to reduce costs in obtaining biomaterials. The purpose of the present study was to compare hydroxyapatite obtained from commercial calcium source and from Colossoma macropomum fish bone through the physical-chemical characteristics and in vitro tests. The materials were characterized by X ray diffraction (XRD), scanning electron microscopy (SEM) and Fourier Transform Infrared Spectroscopy (FT-IR). The sample were treated at 800°C and the XRD results indicated the presence of only hydroxyapatite for the samples obtained from fish bones indicating the purity and stability of the material. The FTIR analysis showed the presence of various functional groups such as* PO_4^{3-}, CO_3^{2-} *and* OH^- *corresponding to HAp. SEM observation confirmed the morphology of the samples to be rod-like and spherical-like. The cell viability and bioactivity of the materials were evaluated by testing the reduction of rezasurin and McCoy medium assay, respectively. The materials did not have a toxic effect and the sample obtained from the fish bone was more bioactive compared to hydroxyapatite from commercial calcium source. It was found that natural HAp exhibited better structural properties compared with synthetic HAp. Therefore, the bio-wastes from fish bone can be utilized in the obtainment of hydroxyapatite which can serve as an alternative for the conventional chemical method getting HAp with good properties and promising application in the biomedical area* **.**
Keywords: *hydroxyapatite, fish bone, biomaterial, in vitro assay, bio-waste.*

1. INTRODUCTION

Hydroxyapatite can be obtained by chemical reactions using different reagents that contain the calcium and phosphate ions, using synthetic or natural calcium sources, such as hen's eggshells (Horta *et al*., 2020; Núñez *et al*., 2018), shells, corals (Wu *et al.*, 2019; Wu *et al*., 2017), etc. Hydroxyapatite can also be extracted from biogenic sources, such as bovine bones, pig bones, camelus bones (Jaber *et al.*, 2018; Ramesh *et al.*, 2018), fish bones and scales (Panda *et al.*, 2014; Horta *et al.*, 2021). Hen's eggshells, fish bones and scales become interesting source of calcium since they are abundant and accessible, reducing the costs of raw materials and bringing environmental benefits with the use of these residues (Sadat-Shojai *et al.*, 2013; Murakami *et al., 2007)*). If these materials are improperly discarded, the organic matter present favors the growth of bacteria and fungi (Rivera *et al.*, 1999), generating undesirable consequences such as bad smell and the occurrence of disease vectors. The great interest in hydroxyapatite (HA) as a biomaterial is related to the mineral phase

of teeth and bones, in which the Hap represents 30 to 70% in mass of hard tissue (Dorozhkin *et al.*, 2010). These data demonstrate the reason for its high biocompatibility and similarities with some properties of bone, including bioactivity, biodegradability and osteoconductivity (Dorozhkin *et al.*, 2010).

This study aimed to obtain hydroxyapatite from *Colossoma macropomum* bones, a typical freshwater fish from Brazil, and compare the material obtained with synthesized HAp. The powders obtained were characterized and tested in vitro to assess cytotoxicity and bioactivity.

2. METHODOLOGY

2.1 Synthesis of hydroxyapatite by precipitaion method

The Ca/P stoichiometric ratio of 1.67 was used for to obtain 5g of HA. The reaction was performed under constant stirring at room temperature. The pH was maintained in the range of 10-12 (Lynn *et al.*, 2002) and corrected with ammonium hydroxide (ProQuimico) when necessary. The calcium hydroxide ($Ca(OH)_2$) solution was previously prepared and stirred for 30 minutes to ensure the homogeneity of the medium. The phosphoric acid (H_3PO_4) solution was added at a rate of 3.33 $mL.min^{-1}$ (Ibrahim *et al.*, 2015) using a peristaltic pump (Milan-model 626). After the adding acid, the solution was aged at room temperature for 1 h under constant stirring and then filtered and washed with distilled water to obtain a white precipitate that was dried at 100 °C/5 hours. This sample was coded as sHA.

2.2 Extraction of hydroxyapatite from *Colossoma macropomum* bones

The *Colossoma macropomum* bones were collected from the local fish market in Manaus city, Amazonas, Brazil. The bones were washed using tap water and the excess meat was removed manually. Then they were boiled in distilled water for 1 h to complement in the material cleaning step. Afterwards, the washed fish bones were treated with 1% (w/v) NaOH solution and heated at 90 °C for 5 h with stirring to remove all organic matter (lipids, proteins), then the powder formed was washed with distilled water for the complete removal of the NaOH solution. Thereafter, the powder (treated bones) was dried at 100 °C/4h, crushed with pistil and mortar and stored. The material was calcined at 800 °C and coded as FBHA.800.

2.3 Characterization

The samples morphological characteristics were investigated using scanning electron microscopy (SEM), model JSM-7100F (JEOL), operating on high vacuum modes, with electron beam potential between 1 and 15kV. For phase identification, the samples were analyzed by X-ray diffraction in a PANalytical diffractometer, model X´Pert PRO MPD, with CuKα copper radiation, $\lambda = 0.155418$ nm with 40 kV voltage and 40 mA current. The scan was $2\theta = 10°\text{-}80°$, at a step size of 0.05° and acquisition rate of $2.5°min^{-1}$. The diffractograms were refined in TOPAS software-Academic program, version 4.0 using Rietveld method to determine the phase compositions and the crystallite size. Fourier Transform Infrared Spectroscopy (FTIR) analyses were performed in a Perkin Elmer Spectrum Two spectrometer. The transmission spectra were obtained in the range 4000 to 400 cm^{-1} and resolution of 4 cm^{-1}.

2.4 In vitro assay

The powders of the samples sHA and FBHA.800 were pressed to form pellets (10 mm) using 150 mg of materials in a hydraulic press (Protécni) at a pressure of 17.75 kgf/cm^2. The samples were sterilized by ethylene oxide. The cytotoxicity test was performed on dental pulp stem cells by resazurin reduction assay according to ISO 10993-5 (2009). The cells were cultured in DMEM (Sigma-Aldrich), with 4500 $mg.L^{-1}$ glucose, in the presence of 10% FBS (Gibco), and 1% Penicillin/Streptomycin (Sigma-Aldrich) at 37 ºC in a humidified atmosphere of 5% CO_2 incubator. The samples extracts were obtained by incubating 0.1 g of dry material per mL of culture medium for 24h (group 1) and 48 h (group 2) in the incubator at 37 °C, 5% CO_2 atmosphere. The cells were seeded at a density of 4×10^4 cells/well in a 96-well plate and cultured for 24 h to allow cell adhesion. After 24 h, the cells were incubated with 100 µL of the extracts for more 24 h (37 °C, 5% CO_2, humidified atmosphere). For positive viability reference (positive control), it was used supplemented culture medium, while 50% (v/v) of dimethyl sulfoxide (DMSO) with supplemented culture medium was used as negative reference (negative control). All experiments were performed in triplicate. After the incubation period, the extracts were replaced for 200 µL of resazurin solution (Sigma-Aldrich) (0.5 mg/L resazurin in PBS, diluted in standard culture medium at 50% v/v) (Souza *et al.*, 2019). The cells were incubated again for 4 h. After incubation, 100 µL aliquots were collected and transferred to another 96-well plate, where fluorescence analysis was performed on a spectrophotometer with a microplate reader (Biotek Synergy HT) at wavelengths of 530 nm excitation and 590 nm emission. The percentage of viable cells was calculated from the average values of absorbance for each sample in relation to the positive control defined as 100% according to Equation 1, where “OD sample” is optical density and “OD cont.+” is optical density of positive control. Then the mean and standard deviation were calculated (mean ± SD). For bioactivity assessment, the cHA

and FBHA.800 pellets were immersed in 16 mL McCoy`s 5A (Horta *et al.*, 2020; Lee *et al.*, 2011) (Vitrocell) medium in Falcon tubes with in aseptic conditions using laminar flow hood. The samples were maintained at 37 °C under 5% CO_2 atmosphere, in an incubator (PANASONIC, COM-19AIC-PA model) for 3 and 7 days (Bonadio *et al.*, 2017). The solution was changed every 3 days. After the incubation period, the pellets were washed with deionized water and dried at 37 °C/24h, then they were analyzed by SEM.

$$\%\ cell\ viability = \frac{OD\ sample}{OD\ Cont.+} \cdot 100 \quad (1)$$

3. RESULTS AND DISCUSSIONS

Figure 1(a) shows the diffractograms results of the sHA and FBHA.800. The diffractograms were refined by the Rietveld method, obtaining the phases quantification and the crystallite size. The XRD patterns showed for both samples an apatite structure according to ICSD 34457 correspond to hydroxyapatite, with crystallite size of 16.67 and 58.62 nm. There was no formation of secondary phases.

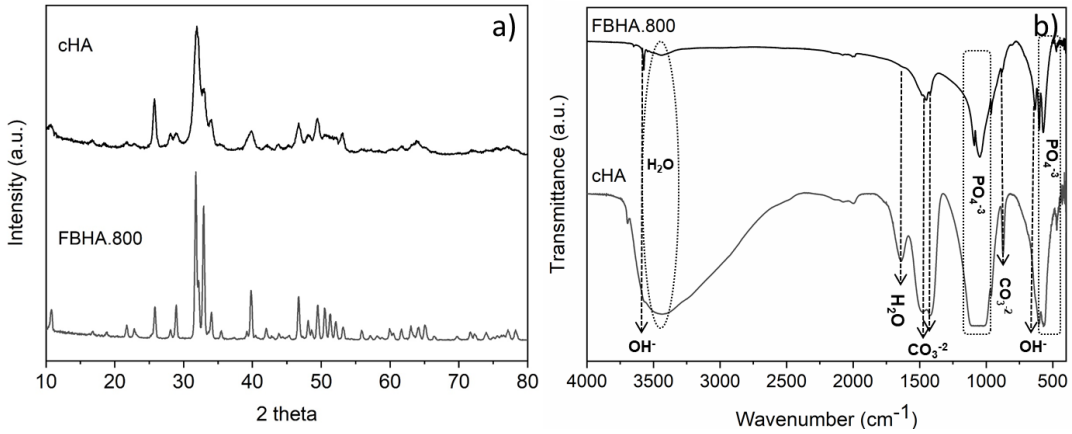

Figure 1. Schematic diagram of the control strategy.

Through FTIR analysis was possible to identify the functional groups present in the HAp powder obtained. The FTIR results (Figure 1(b)) show similar spectra for both samples at around 3000–3700 cm^{-1} which are characteristic of the OH^- stretching of H_2O. A second region referring to the OH^- of H_2O band can be seen in 1641cm^{-1} less intense in the FBHA.800 sample. The regions at 1120–1028 cm^{-1} and 470 cm^{-1} contain the peaks due to the PO_4^{3-} stretching mode. The bands at 958, 563 and 603 cm^{-1} are the characteristic peaks of PO_4^{3-} bending mode. The small bands spotted 3567–3574 cm^{-1} were due to stretching vibration of OH^- groups. The bands at 872, 1415 e 1455 cm^{-1} were due to the presence of carbonate. The presence of carbonated groups is common in biological HAp, with the highest concentration, from 4 to 6% of ions (Dorozhkin *et al.*, 2010), making the samples analogous to biological apatites. The carbonate substitution is particularly important for the mineral phase of bone and has proven to have osteointegration, good biocompatibility and earlier bioresorption compared to normal HAp (Boanini *et al.*, 2010; Sanosh *et al.*, 2009). The bands obtained for the respective phosphates and hydroxyl groups of HAp are in accordance with the data reported in the literature (Othmani *et al.*, 2012; Ramesh *et al.*, 2016). Characteristic groups of organic material were not identified in the FBHA.800 sample, which reflects a good treatment of the sample.

The SEM micrographs of the HAp powder are shown in Figure 2. Scanning electron microscopy was used to analyse the morphology and surface of the samples. The cHA sample has rod-like morphology. This morphology has been reported by different authors (Sanosh *et al.*, 2009; Molino *et al.*, 2020) being a common morphology for the synthesis conditions used. The FBHA.800 is composed of spherical particles and presents a larger size in relation to the other. The morphology was reported by Zainol *et al.*, (2019) for HAp obtained from tilapia fish scales. And all the samples have smooth surface. Inserted in Figure 2(b) there is an image of the fish bones used in this work.

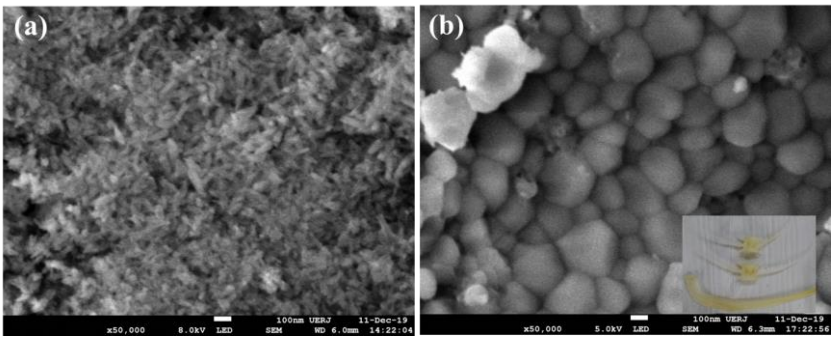

Figure 2. Scanning electron microscopy images for (a) cHA and (b) FBHA.800 samples.

Figure 3 shows the bioactivity assay results for the samples analysed. The McCoy solution was used to simulate the physiological conditions with typical concentrations of ions in the human body (under controlled conditions of pressure, temperature and atmosphere) to evaluate characteristics such as dissolution, morphology and the formation of the bone like apatite layer on the surface of the samples (Bohner *et al.,* 2009).

The cHA sample showed the formation of grooves after 3 and 7 days of immersion in McCoy medium (indicated by white arrows). Nevertheless, the deposition of the *bone like apatite* layer was not verified. The formation of grooves is due to the release of material into the environment. Greater resorption of these samples was already expected, since they have relatively low crystallinity and small crystallite size, as observed in the XRD results. Inserted in the figure there is a micrograph in the same magnification of the FHHA.800 sample after 7 days of immersion for comparison. The literature reports works with different times of immersion, like 3, 7, 14, 21 and 28 days (Bonadio *et al.*, 2017; Zima, 2018; Deb *et al.,* 2019). For the incubation period used in this work, the FBHA.800 sample presented after 7 days of immersion, the beginning of the formation of the apatite layer showing a faster response time compared to synthesized hydroxyapatite.

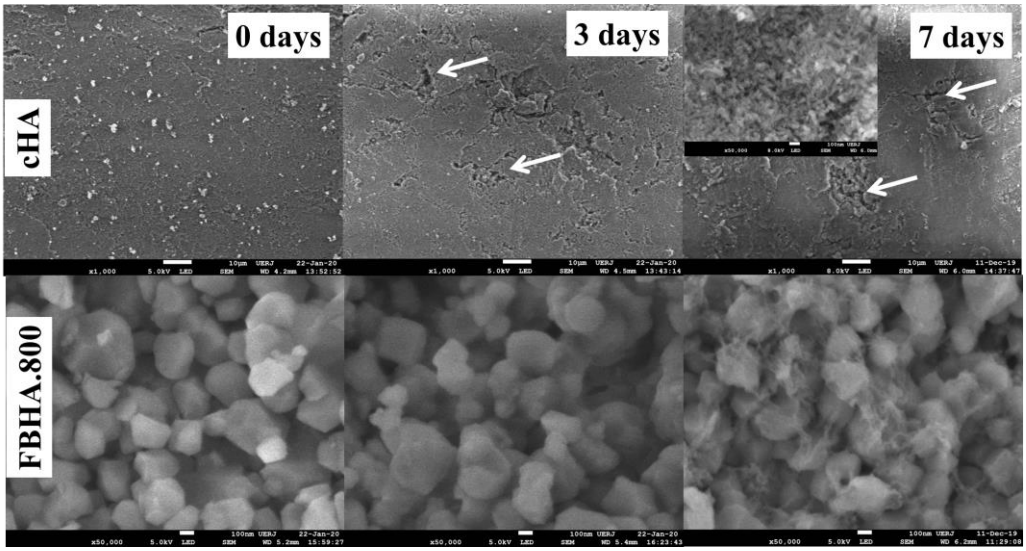

Figure 3. Micrography of samples cHAp and FBHA.800 before (0 days) and after (3 and 7 days) periods of immersion in McCoy solution. The arrows indicate the grooves formed due to the dissolution process Schematic diagram of the control strategy.

The indirect contact assay was performed using extracts obtained for 24h (group 1) and 48h (group 2) of cHA and FBHA.800 samples. The extracts were tested to dental pulp stem cells by resazurin reduction assay evaluated the metabolic function and cellular health. In Figure 4 are presented the results after 24h of incubation.

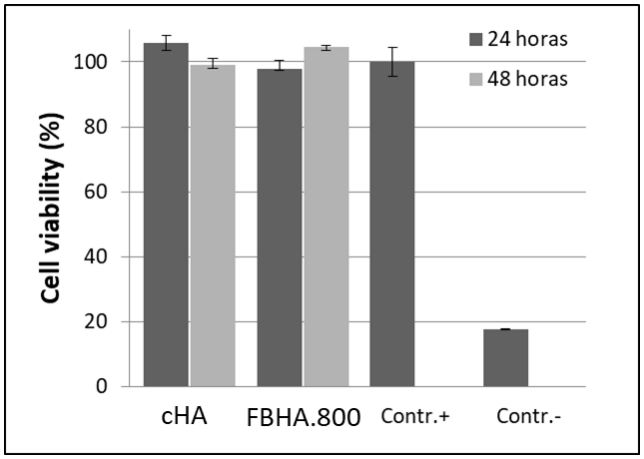

Figure 4. Indirect cytotoxicity of the samples cHap and FBHA.800 to dental pulp stem cells for a 24h incubation period. Cell culture with standard supplemented culture medium was used as positive control (Contr.+) and with 50% (v/v) DMSO in PBS as negative control (Contr.-) of toxicity.

The cell viability for the extracts obtained for the 24h period were 105.7 ± 2.6% and 96.7 ± 2.7% for the samples cHAp and FBHA.800, respectively. And for the extracts obtained for the 48h period, the viability were 98.9 ±2.2% and 104.6 ±0.4% following the same order as the previous one. The values of 105.7% and 104.6% for the cHA and FBHA.800 samples is an indication of increased cell activity resulting from cell growth since cell viability was greater than 100% of the positive control. According to ISO 10993-5 (2009), the reduction of cell viability by more than 30% is considered a cytotoxic effect, thus, no cytotoxicity to dental pulp stem cells was observed for any samples because the percentages of viable cells were above 96%. Researches with different biogenic sources such as bovine bone and shells showed superior results to synthetic HAp from commercial sources (Miculescu *et al.*, 2018; Sun *et al.*, 2017) as well as the results obtained in this work. Such results show that the calcium phosphate compounds obtained from natural sources present similar and/or superior results to those presented by samples synthesized from commercial calcium sources.

4. CONCLUSIONS

HAp from natural source was successfully obtained. The results of the *in vitro* assays provide evidence that the HAp obtained from the fish bone is a strong candidate for raw material to be used in the area of biomaterials, since the results obtained were superior or similar to those of the synthesized HA, for example, FBHA.800 sample showed a better bioactivity compared to the synthesized sHA sample, and also values greater than 100% cell viability. This work is the first record in the literature regarding the use of the *Colossoma macropomum* fish bones, and the results obtained reinforce the use of bio-sources to obtain hydroxyapatite to application as biomaterial, in order to obtain materials with low production costs and relatively simple techniques.

5. ACKNOWLEDGEMENTS

The authors would like to acknowledge FAPERJ (Fundação Carlos Chagas Filho de Amparo a Pesquisa do Estado do Rio de Janeiro, CNPq (Concelho Nacional de Desenvolvimento Científico e Tecnológico) and CAPES (Coordenação de Aperfeiçoamento de Pessoal de Nível Superior) for the grants, and the institutions UFRJ, Estácio de Sá University, NANOFAB/UERJ, LABC/UNICAMP, CBPF and the company R-Crio cryogenics for their cooperation and support for the paper.

6. REFERENCES

Boanini, E., Gazzano, M., and Bigi, A., 2010. Ionic substitutions in calcium phosphates synthesized at low temperature. Acta biomaterialia, v. 6, n. 6, p. 1882-1894.

Bonadio, T. G., Freitas, V. F., Tominaga, T. T., Miyahara, R. Y., Rosso, J. M., Cótica, L. F., ... and Bhalla, A. S., 2017. Polyvinylidene fluoride/hydroxyapatite/β-tricalcium phosphate multifunctional biocomposite: Potentialities for bone tissue engineering. Current Applied Physics, v. 17, n. 5, p. 767-773.

de Souza, R. F. B., de Souza, F. C. B., Rodrigues, C., Drouin, B., Popat, K. C., Mantovani, D., Moraes, Â. M., 2019. Mechanically-enhanced polysaccharide-based scaffolds for tissue engineering of soft tissues. Materials Science and Engineering: C, v.94, p. 364-375.

Deb, P., and Deoghare, A. B., 2019. Effect of acid, alkali and alkali–acid treatment on physicochemical and bioactive properties of hydroxyapatite derived from catla catla fish scales. Arabian Journal for Science and Engineering, v. 44, n. 9, p. 7479-7490.

Dorozhkin, S. V., 2010. Calcium orthophosphates as bioceramics: state of the art. Journal of functional biomaterials, v. 1, n. 1, p. 22-107.

Horta, M. K. D. S., Moura, F. J., Aguilar, M. S., Westin, C. B., Campos, J. B. D., Peripolli, S. B., ... and Archanjo, B. S., 2020. Nanostructured Hydroxyapatite from Hen´ s Eggshells Using Sucrose as a Template. Materials Research, v. 23, n. 6.

Ibrahim, A. R., Zhou, Y., Li, X., Chen, L., Hong, Y., Su, Y., ... and Li, J., 2015. Synthesis of rod-like hydroxyapatite with high surface area and pore volume from eggshells for effective adsorption of aqueous Pb (II). Materials Research Bulletin, v. 62, p. 132-141.

ISO, PNEN, 10993-10995: Biological Evaluation of Medical Devices-Part 5: Tests for In Vitro Cytotoxicity, International Organization for Standardization, Geneva (2009).

Jaber, H. L., Hammood, A. S., and Parvin, N., 2018. Synthesis and characterization of hydroxyapatite powder from natural camelus bone. Journal of the Australian Ceramic Society, v. 54, n. 1, p. 1-10.

Lee, J. T., Leng, Y., Chow, K. L., Ren, F., Ge, X., Wang, K., and Lu, X., 2011. Cell culture medium as an alternative to conventional simulated body fluid. Acta Biomaterialia, v. 7, n. 6, p. 2615-2622.

Lynn, A. K., and Bonfield, W., 2005. A novel method for the simultaneous, titrant-free control of pH and calcium phosphate mass yield. Accounts of chemical research, v. 38, n. 3, p. 202-207.

Miculescu, F., Mocanu, A. C., Stan, G. E., Miculescu, M., Maidaniuc, A., Cîmpean, A., ... and Ciocan, L. T., 2018. Influence of the modulated two-step synthesis of biogenic hydroxyapatite on biomimetic products' surface. Applied Surface Science, v. 438, p. 147-157.

Molino, G., Palmieri, M. C., Montalbano, G., Fiorilli, S., and Vitale-Brovarone, C., 2020. Biomimetic and mesoporous nano-hydroxyapatite for bone tissue application: a short review. Biomedical Materials, v. 15, n. 2, p. 022001.

Murakami, F. S., Rodrigues, P. O., Campos, C. M. T. D., and Silva, M. A. S., 2007. Physicochemical study of CaCO3 from egg shells. Food Science and Technology, v. 27, n. 3, p. 658-66.

Núñez, D., Elgueta, E., Varaprasad, K., and Oyarzún, P., 2018. Hydroxyapatite nanocrystals synthesized from calcium rich bio-wastes. Materials Letters, v. 230, p. 64-68.

Othmani, M., Aissa, A., Grelard, A., Das, R. K., Oda, R., and Debbabi, M., 2016. Synthesis and characterization of hydroxyapatite-based nanocomposites by the functionalization of hydroxyapatite nanoparticles with phosphonic acids. Colloids and Surfaces A: Physicochemical and Engineering Aspects, v. 508, p. 336-344.

Panda, N. N., Pramanik, K., and Sukla, L. B., 2014. Extraction and characterization of biocompatible hydroxyapatite from fresh water fish scales for tissue engineering scaffold. Bioprocess and biosystems engineering, v. 37, n. 3, p. 433-440.

Ramesh, S., Loo, Z. Z., Tan, C. Y., Chew, W. K., Ching, Y. C., Tarlochan, F., ... and Sarhan, A. A., 2018. Characterization of biogenic hydroxyapatite derived from animal bones for biomedical applications. Ceramics International, v. 44, n. 9, p. 10525-10530.

Ramesh, S., Natasha, A. N., Tan, C. Y., Bang, L. T., Ching, C. Y., and Chandran, H., 2016. Direct conversion of eggshell to hydroxyapatite ceramic by a sintering method. Ceramics international, v. 42, n. 6, p. 7824-7829.

Rivera, E. M., Araiza, M., Brostow, W., Castano, V. M., Dıaz-Estrada, J. R., Hernández, R., and Rodrıguez, J. R., 1999. Synthesis of hydroxyapatite from eggshells. Materials Letters, v. 41, n. 3, p. 128-134.

Sadat-Shojai, M., Khorasani, M. T., Dinpanah-Khoshdargi, E., and Jamshidi, A., 2013. Synthesis methods for nanosized hydroxyapatite with diverse structures. Acta biomaterialia, v. 9, n. 8, p. 7591-7621.

Sanosh, K. P., Chu, M. C., Balakrishnan, A., Lee, Y. J., Kim, T. N., and Cho, S. J., 2009. Synthesis of nano hydroxyapatite powder that simulate teeth particle morphology and composition. Current Applied Physics, v. 9, n. 6, p. 1459-1462.

Sun, R. X., Lv, Y., Niu, Y. R., Zhao, X. H., Cao, D. S., Tang, J., ... and Chen, K. Z., 2017. Physicochemical and biological properties of bovine-derived porous hydroxyapatite/collagen composite and its hydroxyapatite powders. Ceramics International, v. 43, n. 18, p. 16792-16798.

Wu, S. C., Hsu, H. C., Hsu, S. K., Tseng, C. P., and Ho, W. F., 2019. Effects of calcination on synthesis of hydroxyapatite derived from oyster shell powders. Journal of the Australian Ceramic Society, v. 55, n. 4, p. 1051-1058.

Wu, S. C., Hsu, H. C., Hsu, S. K., Tseng, C. P., and Ho, W. F., 2017. Preparation and characterization of hydroxyapatite synthesized from oyster shell powders. Advanced Powder Technology, v. 28, n. 4, p. 1154-1158.

Zainol, N. H. Adenan, N. A. Rahim, C. A., 2019. Jaafar, Extraction of natural hydroxyapatite from tilapia fish scales using alkaline treatment. Materials Today: Proceedings, v. 16, p. 1942-1948.

Zima, A., 2018. Hydroxyapatite-chitosan based bioactive hybrid biomaterials with improved mechanical strength. Spectrochimica Acta Part A: Molecular and Biomolecular Spectroscopy, v. 193, p. 175-184.

7. RESPONSIBILITY NOTICE

The authors are the only responsible for the printed material included in this paper.